CLIC Note 104
Note PS/LP 89-16

6. 11. 1989

CLIC TEST FACILITY

THE PHOTOCATHODE TEST BENCH

Y. Baconnier, A Pisent

CONTENTS

CLIC TEST FACILITY

THE PHOTOCATHODE TEST BENCH

Y. Baconnier, A. Pisent

1. INTRODUCTION

The CERN Linear collider (CLIC) idea was first presented in 1986 [1], and accepted as the CERN party line for linear collider studies in 1987 [2]. In 1988 a proposal was made [3] to set up a facility in order to start up a study program on the difficult parts of the injector and to test the RF structures proposed for the drive linac and for the main linac. This proposal was formally accepted and funded in 1989.

One of the facilities to be built is a DC gun and the corresponding beam diagnostic line. This facility is now built and producing its first photoelectrons.

The various people who either have developed or will use this "D.C. test stand" were not familiar with the optics of electron guns and low energy beam lines. This note covers the elementary aspects of these techniques that we had to learn in order to design the equipment and will be needed in order to use it.

2. DESCRIPTION OF THE TEST BENCH

The aim of this test bench is to analyse in detail the behaviour of various photocathodes, gain experience with the use of photocathodes in conditions as close as possible to operational conditions and to compare actual beam optics with existing simulation programs. In a first stage no momentum analysis has been installed. The general layout is given in Fig. 1. A laser beam strikes a photocathode and produces electrons by the photoelectric effect. These electrons are accelerated by a DC high voltage and extracted from the gun through the anode. Their properties are then measured in an appropriate beam line.

2.1 The gun (Fig. 2)

The gun consists of a round photocathode of 8 mm diameter submitted to an electrostatic field of about 80 kV/cm on a gap of 1 cm (8 MV/m). The potocathode is prepared in a preparation chamber which will be the object of a separate note. It is then transferred under vacuum in the DC gun. The anode has a hole in order to let the electrons go through, it is isolated in order to measure the number of electrons lost on the anode.

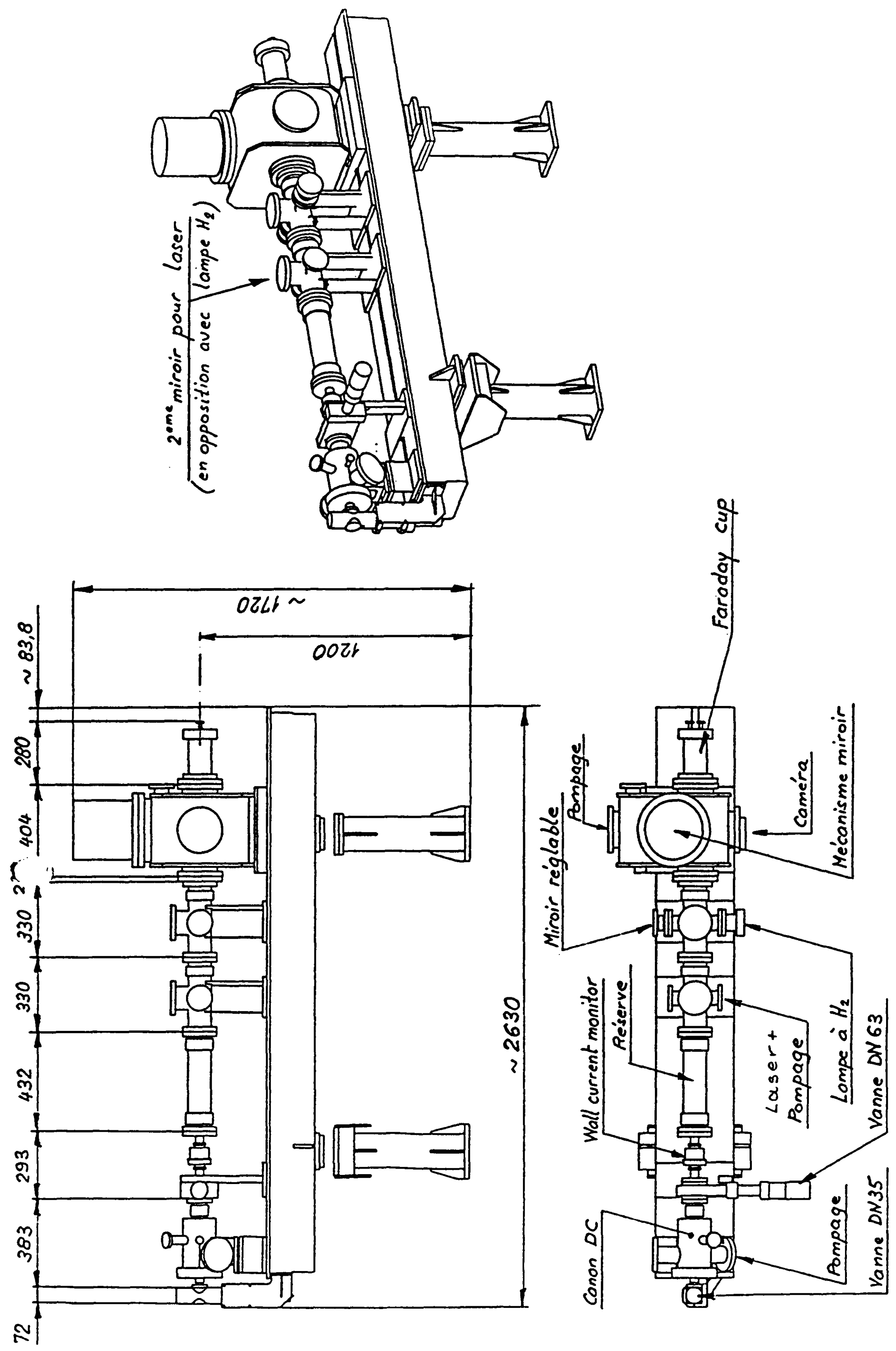

Figure 1: CTF - Test Line

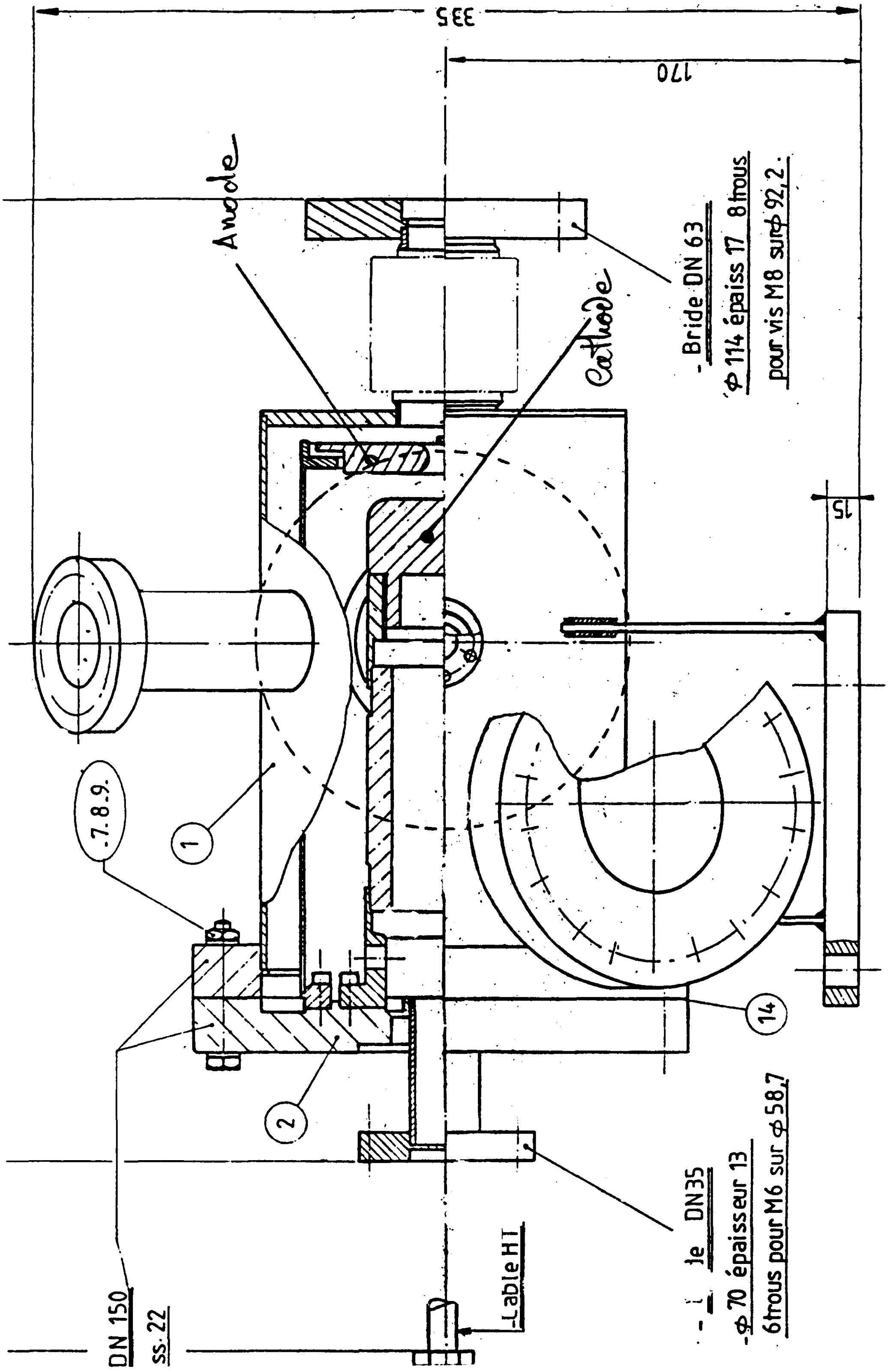

Figure 2: <u>The electron gun</u>

2.2 The beam line (Fig. 1)

Two tanks are foreseen for illumination. One will be used for the introduction of the laser beam. The other tank can be used for direct observation of the photocathode area, for illumination from different light sources, for pumping or for instrumentation. One tank houses the luminescent screens and finally the charge will be measured by a wall current monitor or a Faraday cup.

A set of solenoids is installed in order to contain the beam or to adjust its size at the screen or at the Faraday cup. The first solenoid has been shielded in order not to reduce the field at the photocathode surface. The other solenoids have also been equipped with shields in order to reduce their focal length. The longitudinal position of the solenoids can be adjusted. A list of parameters together with their notation is given in Table I.

2.3 The Solenoids

The first device (that we shall call solenoid of the first kind) has an asymmetric shielding, with an aperture of 65 mm on the cathode side, and 120 mm on the other side. The second and third solenoids are equal (2nd kind); they are symmetric with apertures of 184 mm.

The solenoids fields are well below iron saturation fields, so that we can consider B to be proportional to the current I circulating in the coils. A first idea of the optical propriety of these solenoïds is given by the focal length, calculated as in equation (6).

In Table I are listed the parameters relevant for the dynamics of the beam, at our design energy of 80 kV.

Table I

Parameters of the gun and of the beam line

Gun parameters			
Gap	g	1	cm
Gap voltage	ϕ_g	80	kV
Cathode radius	r_o	4	mm
Solenoid parameters			
First coil			
B_{MAX}/I		135.3	Gauss/A
$\int \left[\frac{B}{B_{MAX}}\right]^2 dz$		5.803	cm
$f\ I^2$ (at 80 kV)		.369	$m.A^2$
Second and third coil			
B_{MAX}/I		74.53	Gauss/A
$\int \left[\frac{B}{B_{MAX}}\right]^2 dz$		9.729	cm
$f\ I^2$ (at 80 kV)		.728	$m.A^2$

3. BEAM OPTICS WITHOUT SPACE CHARGE

The motion of particles in fields with rotational symmetry is described by the well known paraxial equation.

The study of the paraxial equation is a prerequisite in electron gun optics. It is described in various test books [4] [5] but the full demonstration requires some effort. Appendix I details the various steps to obtain the different forms of the equation.

3.1 The gun optics

The optics of the gun can be computed using the paraxial equation (Eq. A.13, Appendix A). In the absence of space charge and without magnetic field it reduces to Eq. (1) where we have used the notations of Lawson [5].

$$\frac{\phi(2\phi_o + \phi)}{\phi_o + \phi} r'' + \phi' r' + \frac{\phi''}{2} r = 0 \tag{1}$$

here, q is the charge of the electron

$q\phi_o$ is the rest energy of the electron

r is the radial position of the beam envelope

$q\phi$ is the kinetic energy

ϕ is the potential along the gap

and the prime denotes a derivation with respect to z the longitudinal coordinate.

Let us consider this equation at the vicinity of the hole in the anode, and note that the longitudinal electrostatic field in the gap E_z is

$$E_z = \frac{\partial\phi}{\partial z} \quad \text{or} \quad E_z = \frac{\phi_g}{g}$$

where g is the gap and ϕ_g the cathode voltage.

We can rewrite this equation under the form

$$\frac{\phi(2\phi_o + \phi_g)}{\phi_o + \phi_g} \frac{\Delta r'}{\Delta z} + E_z \frac{\Delta r}{\Delta z} + \frac{1}{2} \frac{\Delta E_z}{\Delta z} r = 0$$

The field is $E_z = \phi_g/g$ on one side of the hole and zero on the other side so that

$$\Delta E_z = \frac{\phi_g}{g}$$

With the approximation that the radial position does not vary during the traversal of the hole that is $r = cte$, $\Delta r = 0$ we obtain

$$\frac{\Delta r'}{r} = - \frac{1}{2g} \frac{\phi_o + \phi_g}{2\phi_o + \phi_g} \tag{2}$$

and since

$$\frac{\Delta r'}{r} = \frac{1}{f} \tag{3}$$

$$f = 2g \frac{2\phi_o + \phi_g}{\phi_o + \phi_g} = 2g \frac{1 + \gamma}{\gamma} \tag{4}$$

In our case $\phi_g = 80$ kV, $\phi_o = 511$ kV $\qquad f = 3.72\ g = 37$ mm.

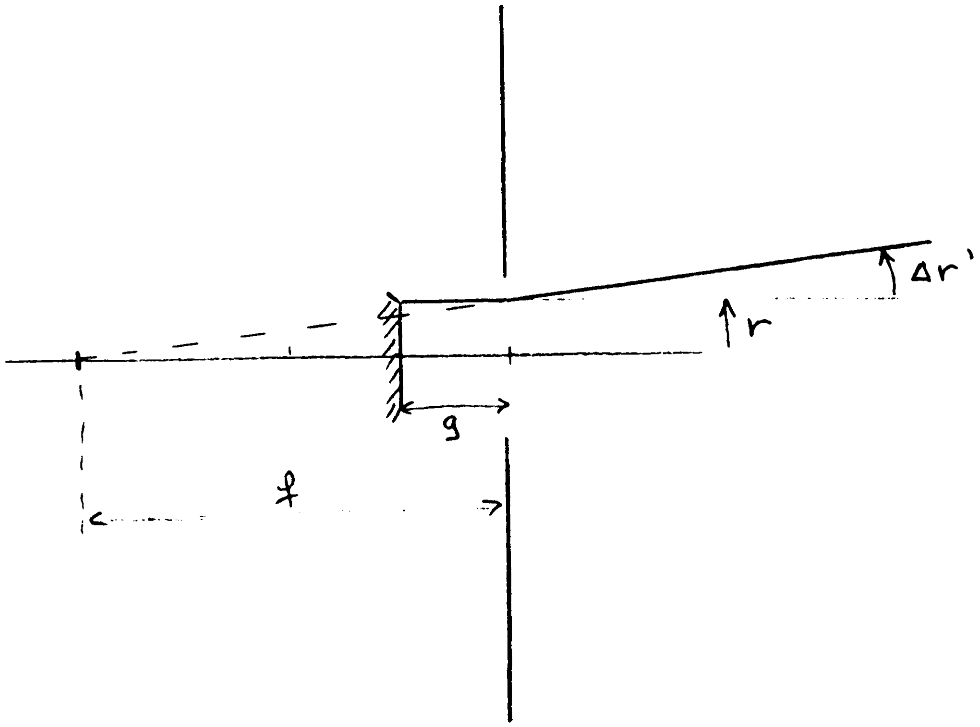

Figure 3: The Gun Optics

3.2 The Solenoids

The solenoids are magnetic lenses. We start with the paraxial equation (A-10) in the case where there is no electric field ($E_z = 0$) so that $z = \beta ct$ and where the particles start with a velocity parallel to the axis in a zero field at a distance r_0 from the axis so that $r_0' = 0$ and $\psi_0 = 0$ (fig. 4). In this case the paraxial equation writes

$$r'' = -\frac{1}{4} r \cdot \frac{B_z^2}{(B\rho)^2} \qquad (5)$$

If during the traversal of the lens r stays approximately constant we have by integration (see fig. 4)

$$\frac{\Delta r'}{r} = -\frac{1}{4}\frac{1}{(B\rho)^2}\int B_z^2 dz = -\frac{1}{f}$$

The magnetic lens constituted by a coil is a focusing lens of focal length

$$f = 4\frac{(B\rho)^2}{\int B^2 dz} \qquad (6)$$

The solenoids parameters [7] are given in Table I.

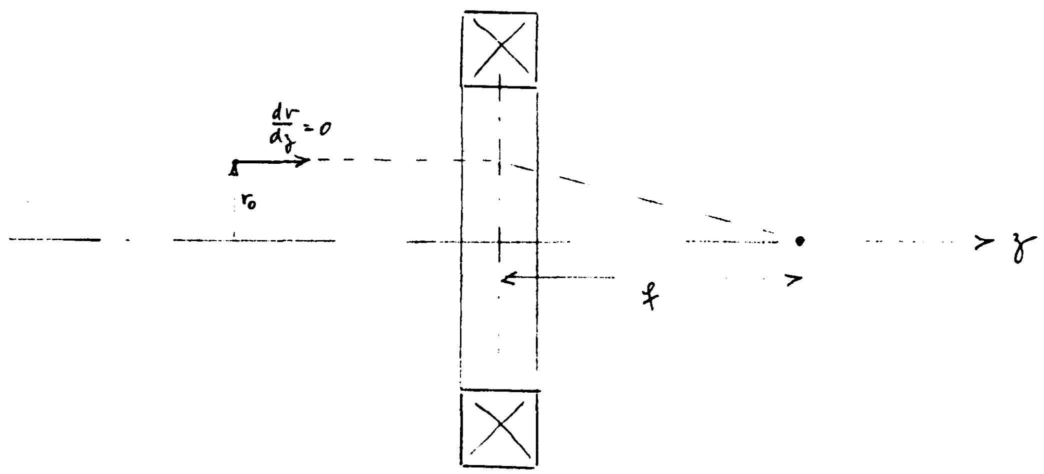

Figure 4: Focal length of a solenoid

3.3 The beam line layout

We have placed the two mirrors for cathode illumination at 1000 mm and 1350 mm from the cathode, the screen at 1730 mm and the faraday cup at 2100 mm (Fig. 5). The position of the solenoïds is given in Table II.

We can compute the required focal length by the optics formula

$$\frac{1}{x_1} + \frac{1}{x_2} = \frac{1}{f}$$

The results are tabulated in Table II.

Table II

Focal length of solenoids (m)

Calculated using geometrical optics

L e n s	x_1(mm)	x_2(mm)	f(mm)	r(mm)	I (80 kV) (A)
Electrostatic	00	- 37	- 37	4	
Solenoïd 1	97	346	76	11	2.20
Solenoïd 2	346	346	173	11	2.05
Solenoïd 3	346	346	173	11	2.05

One can also compute the beam sizes at the position of the various lenses given the radius at the cathode : r_0= 4mm. These values are also listed in Table II.

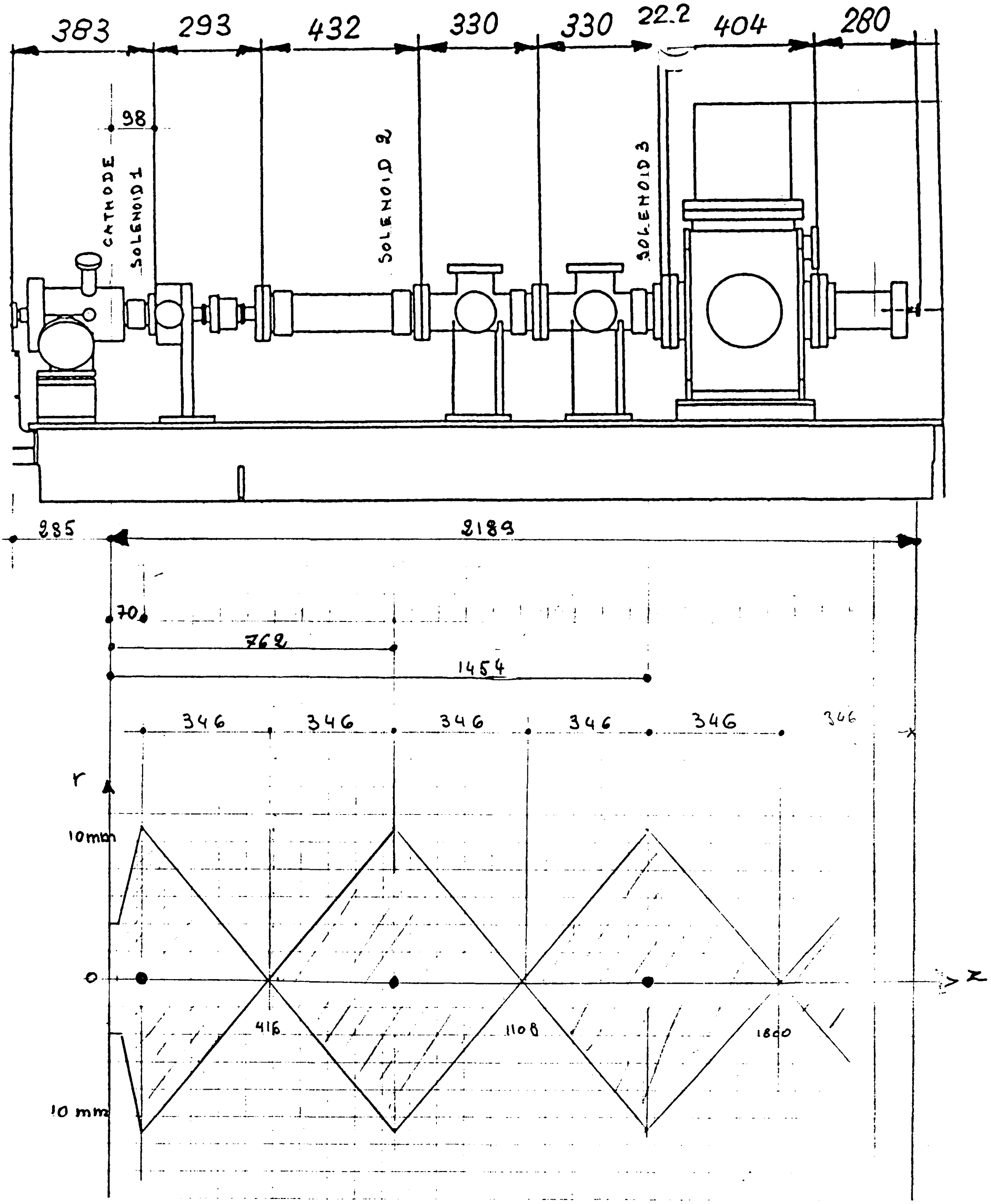

Figure 5: Beam optics in the test bench

4. THE EFFECT OF SPACE CHARGE

In a continuous beam one can use the paraxial equation to compute the trajectories in the presence of space charge. In the general case the integration has to be performed numerically, but a general solution exists in the simplified case of a drift space. This general solution helps to understand the effect of space charge in verious cases.

For what concerns the longitudinal dynamics the one-dimensional problem in an accelerating gap it can be solved analytically; this is again a good indication of the performances the actual geometry can achieve.

4.1 The paraxial equation under space charge conditions

In a continuous beam the paraxial equation can be used to compute the envelope of the beam by computing the electrostatic field and the magnetic field due to the beam and adding the result to the external fields. It is easy, using the Gauss theorem to compute the electric field E_r. The effect of the magnetic field of the beam is introduced via the "relativistic compensation" $1-\beta^2$*. One of the conditions of validity is obviously that the linear density of particles does not vary too much in a distance of the order of the beam diameter.

With these restrictions the paraxial equation (A-10) writes

$$\ddot{r} + \frac{\beta}{\gamma}\frac{q}{m_0 c} E_z \dot{r} + \frac{1}{4\gamma^2}\frac{q^2}{m_0^2} B_z^2 r - \frac{1}{4\gamma^2}\frac{q^2}{m_0^2}\frac{\psi_0^2}{\pi^2}\frac{1}{r^3} - \frac{1}{\beta\gamma^3}\frac{q}{m_0 c}\frac{1}{2\pi\varepsilon_0}\frac{I}{r} = 0 \qquad (7)$$

This equation has been solved by numerical integration in a PC.

4.2 The effect of space charge in drift space [4)8)]

In the particular case where there is no acceleration ($E_z=0$), no magnetic field ($B_z=0$), no angular momentum ($\psi_0=0$) but only space charge we can rewrite the paraxial equation with z as independent variable (A-11):

$$\frac{d^2 r}{dz^2} - \frac{\xi}{r} = 0 \qquad (8)$$

---

* The $1-\beta^2$ coefficient can be obtained directly by calculating the electrostatic forces in the frame of the particles and effecting a Lorentz transformation to the laboratory frame (see E. Keil, CERN 77-13, p. 314 (ref. 11).

with

$$\xi = \frac{1}{\beta^3\gamma^3} \frac{q}{m_0 c^3} \frac{I}{2\pi\varepsilon_0}$$

in our gun $\xi/I = 6\times10^{-4}$ (A^{-1}), or more practical (MKS units):

$$\xi = 2.10^{-7} \frac{I}{(\beta\rho)\gamma^2\beta^2}$$

The solution of Eq. (8) must conserve the quantity W

$$W = \frac{1}{2} \left(\frac{dr}{dz}\right)^2 - \xi \log r \qquad (9)$$

since

$$\frac{dW}{dz} = \frac{d^2r}{dz^2}\frac{dr}{dz} - \xi \frac{1}{r}\frac{dr}{dz} = \frac{dr}{dz}\left(\frac{d^2r}{dz^2} - \xi \frac{1}{r}\right) = 0$$

Note that W is proportional to the transverse energy of the particle, the first term in (9) being the kinetic energy, the second the potential energy.

If we choose the constant to be $W = -\xi \log r_0$, r_0 is the beam size at a minimum *), and we can write the equation :

$$dz = \frac{1}{\sqrt{2\xi}} \frac{dr}{\sqrt{\log \frac{r}{r_0}}} \qquad (10)$$

The solution can be written as :

$$X\, I^{1/2} \left(\frac{z}{r_0}\right) = F\left(\frac{r}{r_0}\right) \qquad (11)$$

with

$$X = \left[\frac{2\xi}{I}\right]^{1/2}$$

and

$$F(y) = \int_1^y \frac{dy}{\log y} \qquad (12)$$

A our energy $X = 34.46\ 10^{-2}$ ($A^{-1/2}$)

---

*) because of (9) it can be either a minimum or a maximum, but the system is defocusing and starts with a converging beam.

One can find the non-relativistic approximation in various books [4) 8)].

$$X_{nr} = \frac{3\times10^4}{\phi_0^{3/2}} = 3.64 \times 10^{-2}\ (A^{-1/2}) \text{ at } 80 \text{ kV} \qquad (13)$$

If we now pose $x = r_0/r$, Eq. (11) becomes :

$$X\ I^{1/2}\ (z/r) = x\ F(1/x) \qquad (14)$$

where the RHS is plotted below.

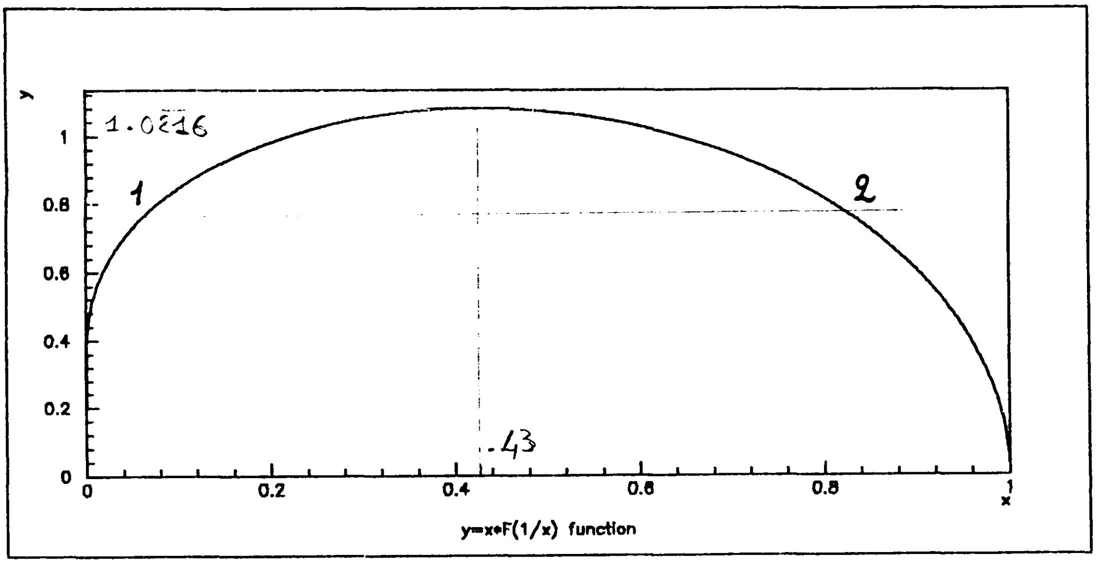

Figure 6: Plot of the function x F (1/x) RHS of eq. 14

We want to transmit a beam with significant space charge; if we consider (Fig. 7)a symmetric configuration and choose $z = 0$ in the middle point equation (14) will describe the relation between r, z and r_0 for a given current I.

From the behaviour of the function x F(1/x) we see that in general we shall have two solutions for r_0 at a given current: (indicated as 1 and 2 in Figure 6).

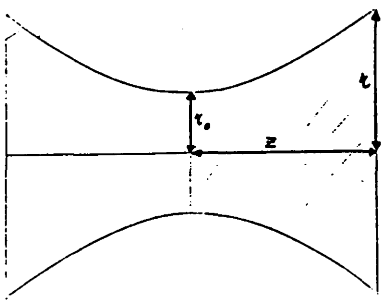

Fig. 7: Definition of r_0, r and z

At the limit of zero current, those two cases correspond to the parallel transmission and to the focusing in the middle point. Increasing the current at x = .43 where x F(1/x) = 1.0816, we will have a unique solution, and then no solution at all. This defines the maximum current :

$$I_{max} = \frac{1.1696}{X^2} \left(\frac{r}{z}\right)^2 \qquad (15)$$

A way "à la mode" to say this, is that our a dynamical system; differential equation plus the boundary we have imposed, has a <u>bifurcation</u> at the value I_{max} of the parameter I.

From Eq. (10) and (14) one can calculate

$$\frac{dr}{dz} = X\, I^{1/2} \sqrt{\log\left(\frac{r}{r_0}\right)} = \frac{r}{z} \left[x\, F\left(\frac{1}{x}\right) \sqrt{-\log x}\right]$$

In particular at the maximum current, x F(1/x) is maximum, i.e.,

$$\frac{d}{dx}\left[x\, F\left(\frac{1}{x}\right)\right] = F\left(\frac{1}{x}\right) - \frac{1}{x} \frac{1}{\sqrt{-\log x}} = 0$$

and then dr/dz = r/z.

In other words if the optics is matched without space charge to have the focus in the middle point of the drift space, the same matching still gives a symmetrical solution for $I = I_{max}$.

If we consider the geometry of Table I (r = 11.5 mm, z = 346 mm) we can calculate I_{max} = 1.08 A; the corresponding computer run using the program SOLOPT [9] confirms that the zero space charge matching is also valid for I = 1.08 A (Fig. 8).

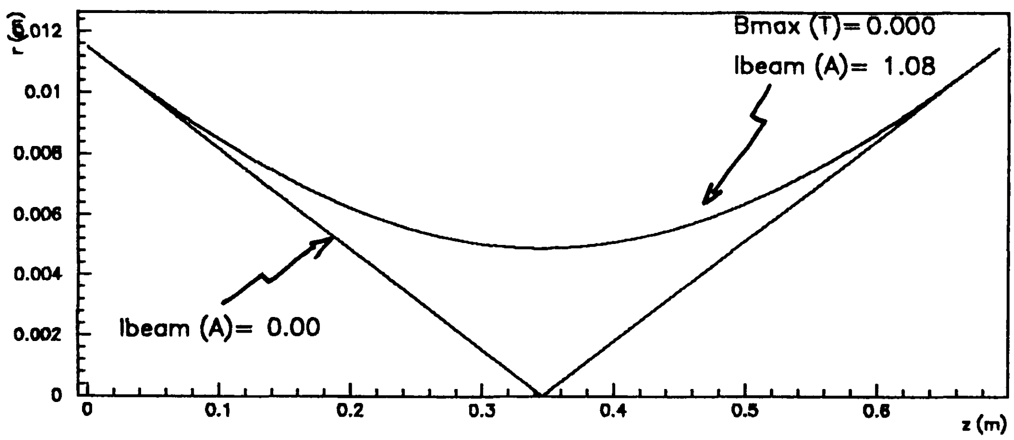

Figure 8: Tracking of beam with I = 0 and $I = I_{max}$ using SOLOPT

4.3 <u>Space charge limited emission</u> (Perveance)

The emission of electrons from a surface can be generated by various processes and then have different intrinsic characteristics and limitations. There is in all cases a limitation due to space charge that is independent from the emission details: when an electron leaves the cathode it feels a backward force due to the charge of the electrons already emitted. If we consider a cathode capable to generate an unlimited number of electrons (with zero kinetic energy) a condition of dynamical equilibrium will be reached when the space charge field exactly counterbalances the external accelerating field, or in other words when the E field at the cathode is null.

The one dimensional problem (two plates indefinitly extended) can be solved exactly [4] and gives

$$\Phi = \Phi_g \left(\frac{z}{g}\right)^{4/3}$$

where Φ is the potential along the beam axis, Φ_g is the gap voltage and g is the gap. Observe that the gradient of Φ is zero at the cathode. The explicit relation between Φ_g and the maximum current I_{max} is

$$I_{max} = K \, \Phi_g^{3/2} \qquad (16)$$

In the case of our one dimensional problem K is only defined per unit area

$$K = \frac{4}{9} \, \frac{\varepsilon_o}{g^2} \sqrt{2 \, \frac{e}{m}} = 2.33 \times 10^{-6} \, \frac{1}{g^2} \qquad (17)$$

The constant K is called perveance of the gun. It is only a function of the geometrical dimensions (being a local propriety in the neighbourhood of the cathode). When $I < I_{max}$ the quantity $K = I/\Phi_g^{3/2}$ is used to define the perveance of the beam.

Our cathode is of limited radial extension, so its behaviour is not well described by the one dimensional approximation (17). At the edge of the emitting area the longitudinal effect of space charge is lower, so that the current distribution is not homogeneous. The practical way to simulate the infinite plane solution is a reshaping of the electrodes called a Pierce type gun [5].

4.4 The difficulty at the cathode

The space charge produces a radial electric field E_r. This field however must be null at the surface of the cathode due to the conditions at a conducting surface. Moreover, the linear density at the vicinity of the cathode varies very rapidly so that the conditions required to introduce the space charge (§ 4.2) are not fulfilled. The proper treatment of the electron motion requires a proper computation of the field using the Poisson equation.

In order to understand the behaviour of the particles at the vicinity of the cathode we can use a simplified model. The cylinder of charge emitted by the cathode and accelerated is replaced by a linear density of particles and its image in the cathode.

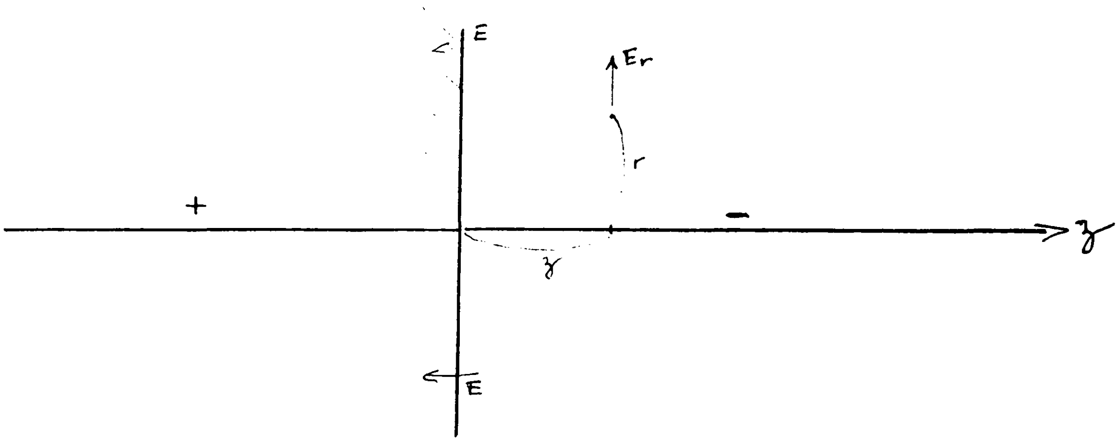

Figure 9: The simplified model of the cathode

If λ is the line density along z the field E_r can be computed by a straightforward integration.

$$E_r = \frac{\lambda}{2\pi\varepsilon_0} \frac{1}{r} \frac{z}{(r^2+z^2)^{1/2}}$$

that is the field due to a constant line density multiplied by a correction factor

$$k = \frac{z}{(r^2+z^2)^{1/2}}$$

This correction factor can be applied to the space charge term of the paraxial equation to approximate the image effects at the cathode. This approximation has been introduced in our PC program.

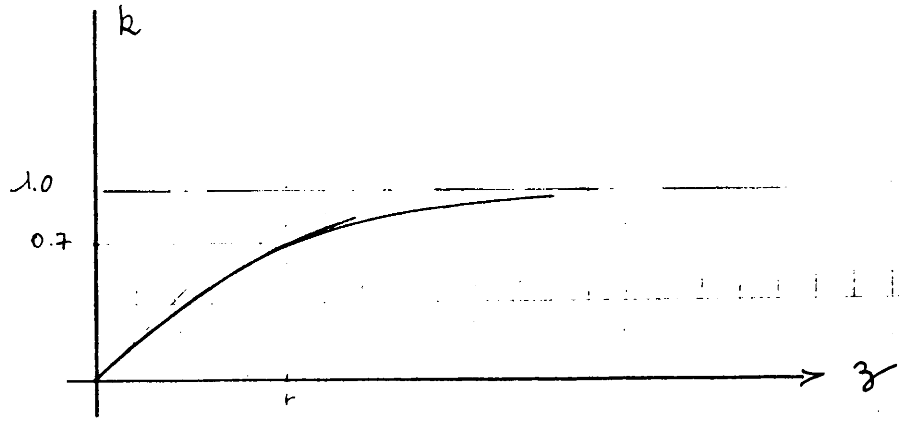

Figure 10: The correction factor R

5. DETAILED COMPUTATIONS

5.1 The paraxial equation

A simple program using a PC has been written to integrate the paraxial equation including the effect of space charge at the vicinity of the cathode and the radial field due to the hole in the anode. The aim was to understand and check the more precise techniques of computations.

The beam line with 3 solenoids has been simulated with zero current in the beam and with a current of 1 A close to the maximum current acceptable in this beam line.

The results are indicated in the Table IV and in Fig. 11, Fig. 12 gives a typical output of the program called PARAXIAL.

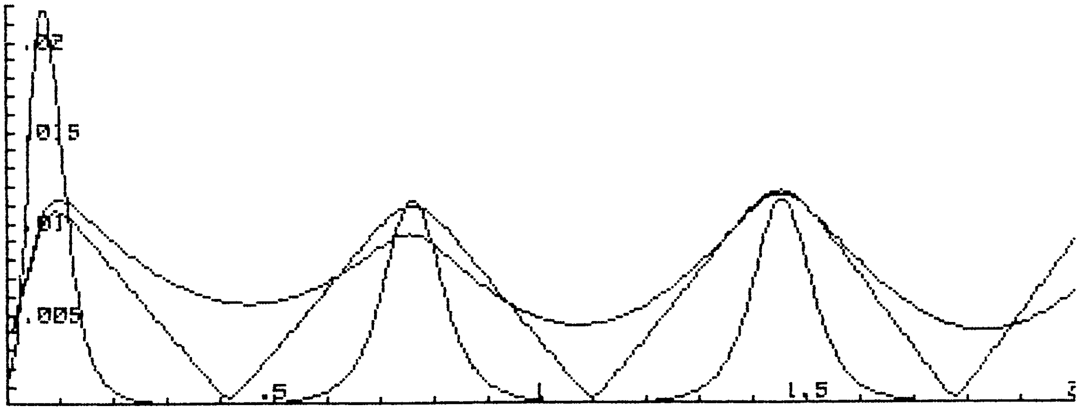

Fig. 11: The beam line with 0 and 1 A

Cathode radius (cm)=	.400	Kinetic energy (eV)=	.2
Charge (nC)=	0.00	Laser pulse (nS)=	10.0000
RprimeO (dr/dz)=	0.000	RthetaprimeO R*dtheta/dz=	0.0
Photoemission			
Quantum efficiency =	.010	Number of Electrons E10	0.000
Cath. Current (A)=	0.00	Current density (A/cm2)=	0.000
Laser power (MW)=	0.000	Laser energy (MicroJoule)=	0.000
First coil			
Foc. length (Foc1)	.065	Current (A) =	2.380
Bmax (Gauss)	322.022	Coil to cathode (cm)=	7.000
Secnd coil			
Foc. length (Foc2)	.151	Current (A) =	2.195
Bmax (Gauss)	163.597	Coil to cathode (cm)=	76.200
Third coil			
Foc. length (Foc3)	.151	Current (A) =	2.195
Bmax (Gauss)	163.597	Coil to cathode (cm)=	145.400
Field at the cathode =	.0017		

Fig. 12: Output of PARAXIAL

5.2 Computer Simulations

To simulate the behaviour of the electrons in a beam line we have used two codes with different characteristics:

- SOLOPT is a short home made code that tracks the beam through the transfer line using TRANSPORT matrices for the solenoids and non-linear kicks for space charge[9]. It assumes laminar motion (for space charge calculations the most external trajectory is considered to be the envelope), a continuous beam and no acceleration. The code is well suited for rapidly adjusting the position and strength of solenoids.
- EGUN [12] is a well known code written to study the optics of an electron continuous beam, with special attention to gun optics design. The main parts are a Poisson solver and a ray tracker, plus various routines to simulate the effect of an external magnetic field; the code calculates the E field without particles, tracks the particles in that field (considering also the external B field), recalculates E and retracks the trajectories, and so on until the result converges. The iteration is done on the current, and cylindrical symmetry is assumed. This code is well suited for the study of the geometry of the cathode, but, with some effort, can be used to track the electrons along all the two meters of the structure.

5.3 The cathode studied with E gun

The space charge limit of our gun geometry has been calculated in the sense explained in chapter 4.3; the limited current is 36A. The anode has been made large enough to let this current go through. (Fig. 13).

With EGUN we have done a systematic study of the conditions in which the beam leaves the cathode, in order to estimate the actual focal length of the electrostatic diverging lens described in chapter 3.1, with and without space charge. Results are listed in Table III. The defocusing lens is stronger than foreseen in thin lens approximation.

TABLE III

Coordinates of the most external electron at z = 30 and resulting focal length for the nominal gap of 1 cm

I (A)	K mA · $V^{-3/2}$	r (mm)	dr/dz	f electrostatic (mm)
0.00	0.0000	7.1613	.1310	34.67
1.00	0.0442	7.2895	.1387	32.56
5.00	0.2210	7.8011	.1609	28.48
10.00	0.4419	8.4470	.1883	24.86

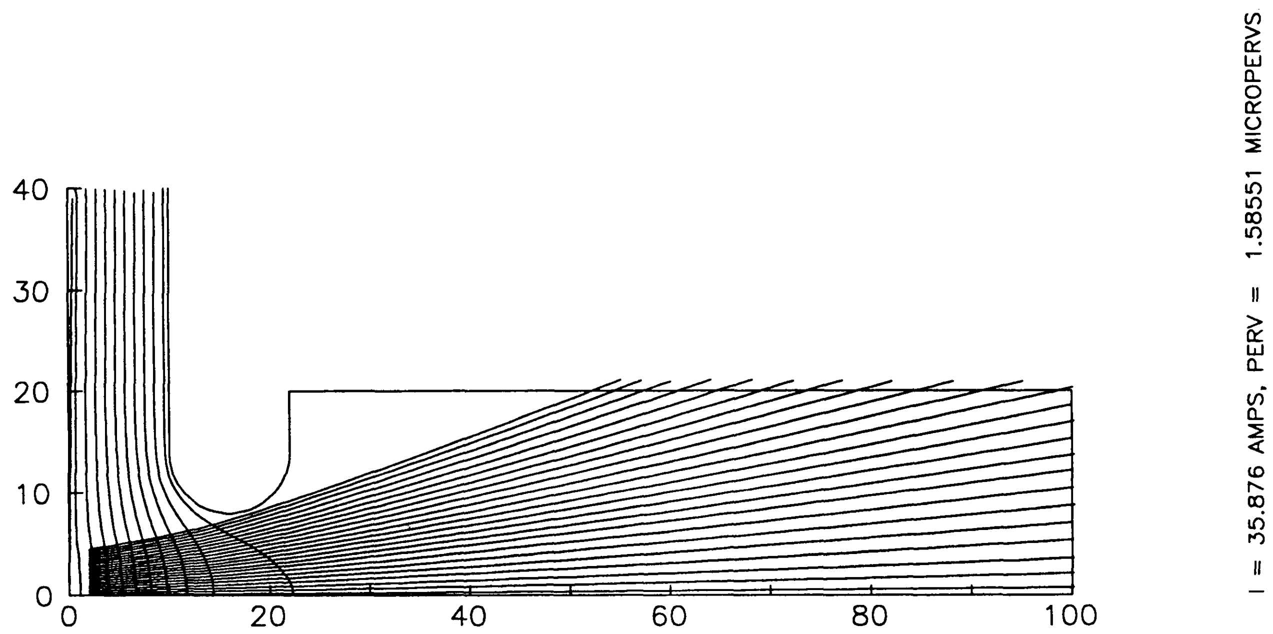

Fig. 13: The cathode at the space charge limit (without magnetic focusing)

5.4 The nominal geometry

The first aim of computer simulations was to fix a nominal geometry, without space charge, but with the field shape of the real solenoids. To get this result, with a satisfactory agreement between the codes used, a careful analysis of the cathode region (first two centimetres) has been necessary.

For the code PARAXIAL the delicate point is the electrostatic lens: the dependence of E_z on z is far to be a step function, and the electrons are focalized also before reaching the energy $q\phi_g$.

To have an accurate description of the dynamics the potential $\phi(z,r=0)$, calculated by the POISSON solver of EGUN has been introduced.

SOLOPT instead is a transport code and the acceleration process has previously to be described by EGUN. With the chosen mesh-size of 1 mm the code of SLAC can cover in one run around 30 cm, modelizing acceleration and magnetic focusing; each point after the gap can be chosen as initial point for the SOLOPT run. In the runs presented in this paper this "gluing" point is located at 22 mm from the cathode (end of the anode). In such a way it is possible to separate the magnetic focusing from the electrostatic defocusing, calculated once for ever with a series of runs of EGUN. The dependence of (r, r') at z = 22 mm as a function of the beam current is linear in good approximation. SOLOPT is then enough to adjust the solenoid strengths. The error introduced in this separation of electrostatic and magnetic effect, minimized with the choice of the 22 mm, can be evaluated in some percent (due mainly to the electrostatic lens).

In table IV the nominal optics found with the two approaches are shown. Fig. 14 shows the beam layout and Fig. 15 the EGUN simulation of the cathode region.

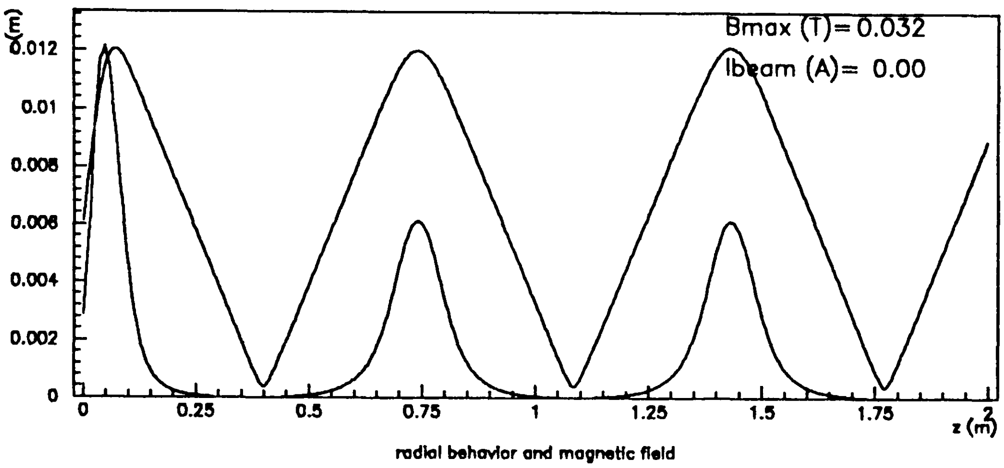

Fig. 14: The nominal optics

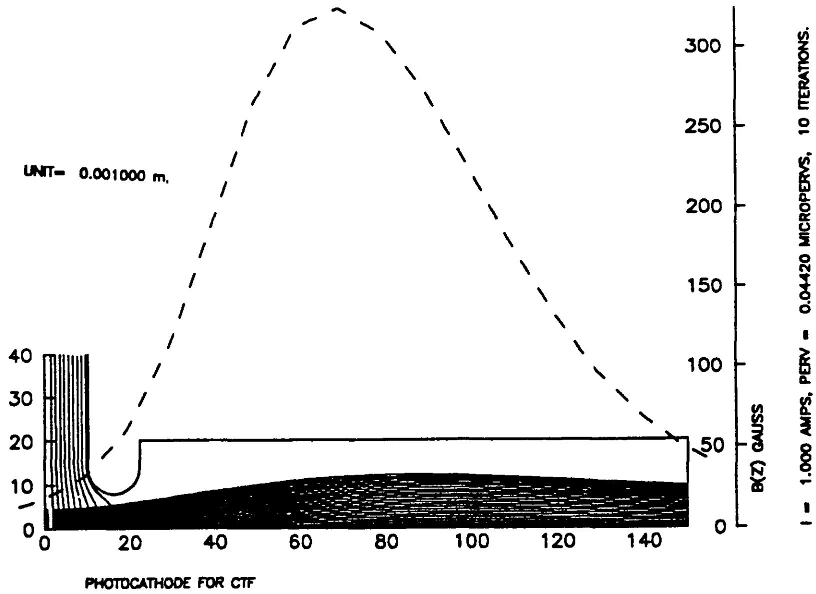

Fig. 15: The beam behaviour at the cathode (1 A)

T A B L E IV

The nominal optics

Solenoid kind	z (mm)	PARAXIAL I (A)	SOLOPT I (A)
1	70	2.380	2.394
2	762	2.195	2.200
2	1454	2.195	2.200

5.5 The space charge effect

Analyzing now the effect of space charge it has been shown in paragragh 4.2 that the drift spaces between the first and the second, and between the second and the third solenoid admit a maximum current of about 1 A with a symmetrical configuration; this occurs keeping the focal strength of the zero current case.

Our geometry is more complicated, being the beam dimension at the first coil a function of the current; in the very simplified hypothesis of thins lenses and a linear dependence:

$$r = r_0 + \alpha I$$

the equation (15) which determines I_{MAX} becomes the quadratic:

$$I = \frac{1.1696}{X^2 Z^2} (r_0 + \alpha I)^2$$

For the parameters of the nominal optics (r_0 = 12 mm, α = .1 mm/A) the maximum current is 1.3 A. For this value the beam shape should be the same in each drift space. Using thick lenses instead the electron ray is quite asymmetric in the first coil (the maximum occurs some centimeters after the coil center) and so the behaviour is not completely regular (fig. 15).

If the 1 A limit is a good indication of the performances of the line, it is not at all the ultimate limit. In fig. 16 we show a possible layout for a beam current of 5 A: the beam is kept small at the beginning where is located the Wall Current Monitor, and in the position of the mirror of the laser. Where the chamber is large instead the beam expands to 35 mm.

5.6 The effect of the field at the cathode

In the configuration presented, with a solenoid of the first kind at 70 mm from the cathode, the field at the emission point is $B_0 = 0.54 \; B_{MAX}$, i.e. of around 18 Gauss at the nominal solenoid current. The memory of this field is kept all along the line.

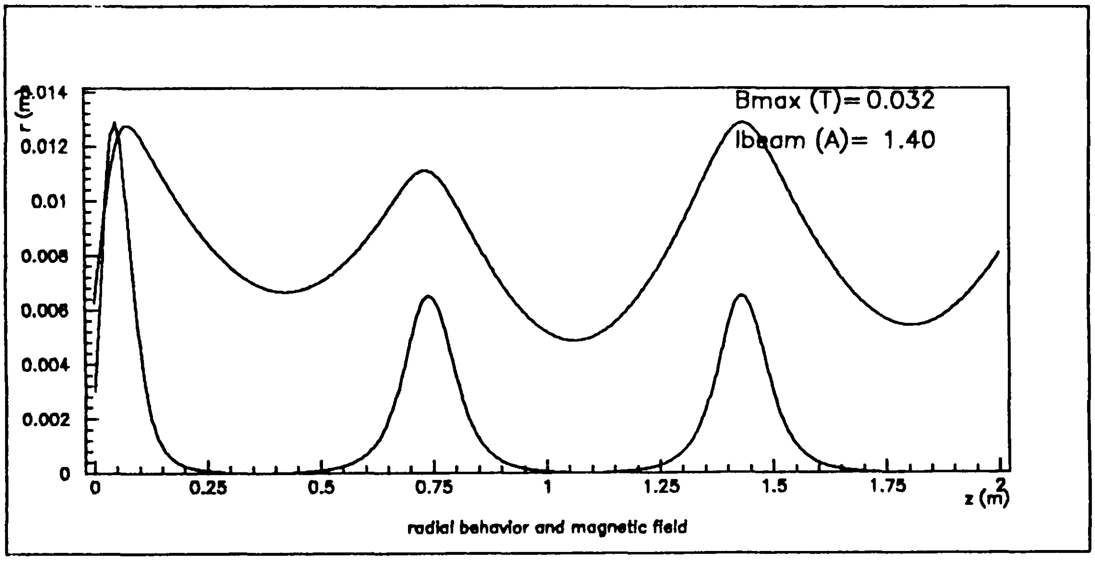

Fig. 15: Beam behaviour at 1.4 A

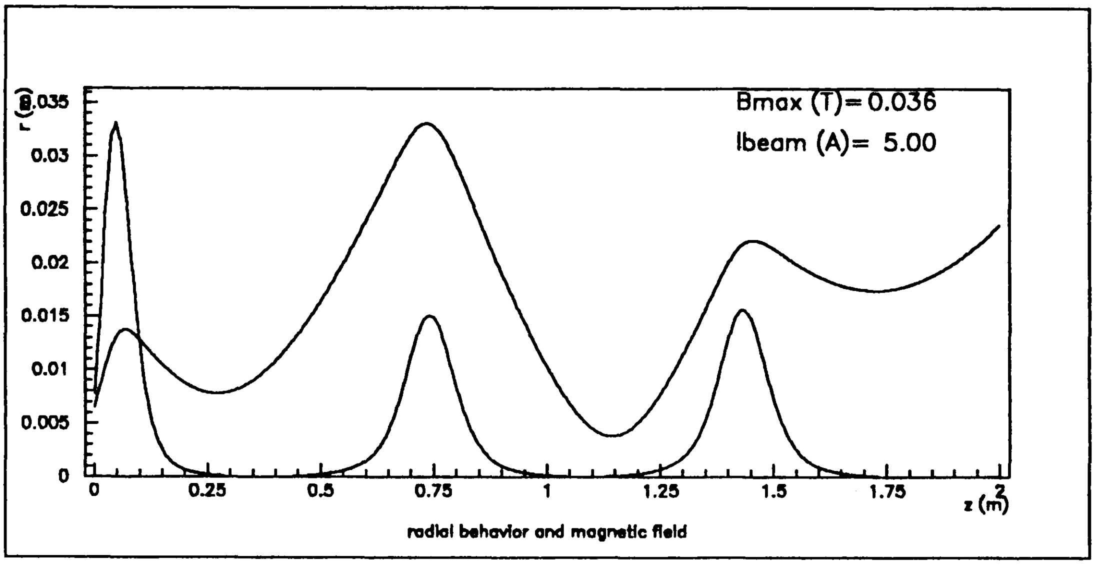

Fig. 16: Beam behaviour at 5 A

In fact, if the electron is observed at a point with B = 0, Bush theorem (A-6) prescribes it to have an angular velocity

$$\dot{\theta} = \frac{q\ B_0}{2\ m} \left[\frac{r_0}{r} \right]^2$$

that weakens the focusing of all the solenoids met along the line. Fig. 14 shows that this effect on the beam is very weak (namely r is not exactly zero at the focuses); the shielding provided at the first solenoid looks then adequate.

Acknowledgements

We want to thank E. Jensen for the installation of the code EGUN on CERNVM and for continuous advice on its use.

References

1. W. Schnell, A Two Stage RF linear collider using a superconducting drive linac, CLIC Note 13, February 1986.

2. K. Johnsen et al., Report of the Advisory Panel on the projects for e^+/e^- linear colliders in the TeV range, CERN 87-12, May 1987.

3. Y. Baconnier et al., A CLIC injector test facility, CLIC Note 65, June 1988.

4. J.R. Pierce, Theory and design of electron beams (2nd ed.), Van Nostrand, Princeton, NJ. 1954.

5. J.D. Lawson, The physics of charged particle beams, Clarendon Press, Oxford (2nd edition)), 1978.

6. F. Rohner, Solenoids for the CTF, PS/PA Note 89-15, June 1989.

7. E. Keil in Proceedings of the 1976 Erice School, CERN 77-13.

8. R. Hutter in: Septier, Focusing of charge particles, Academic Press, New York (1967).

9. A. Pisent, SOLOPT: a transport code with space charge in a solenoid field, Note PS/LP 89-29.

10. E. Durand, Electrostatique et Magnétostatique, Masson, Paris (1953).

11. W.B. Hermannsfeld, SLAC-331, 1988.

12. H. Bruck, Accélérateurs de particules, P.U.F., 1966.

13. C. Bovet et al., A Selection of formulae and data useful for the design of AG Synchrotrons, CERN/MPS-SI/Int. DL/70/4 (1970).

Appendix I

The paraxial equation is the equation of motion of particles. equating the time derivative of momentum to the force

$$\frac{d\vec{p}}{dt} = q\,(\vec{E} + \vec{v} \times \vec{B}) \qquad \text{(A-1)}$$

in the particular case of systems with axial symmetry and with simplified field configurations and in the hypothesis of a velocity almost parallel to the axis z.

The system of coordinates is r, Θ, z (fig. 1). Several textbooks give the development of eq. 1 in cylindrical coordinates. One can find a detailed derivation in Bruck [12] page 28. Using the notation of Bruck this is

$$\left.\begin{aligned}
&\frac{d}{dt}(m\dot{r}) - m\,r\,\dot{\Theta}^2 = q\,(E_r + r\,\dot{\Theta}\,B_z - \dot{z}\;B_\Theta) \\
&\frac{1}{r}\frac{d}{dt}(m\,r^2\,\dot{\Theta}) = q\,(E_\Theta + \dot{z}\,B_r - \dot{r}\,B_z) \\
&\frac{d}{dt}(m\dot{z}) = q\,(E_z + \dot{r}\,B_\Theta - r\,\dot{\Theta}\,B_r)
\end{aligned}\right] \qquad \text{(A-2)}$$

This is a relativistic equation so that $m = \gamma\, m_o$ varies in time due to the acceleration by E_z.

We consider a configuration of fields with axial symmetry where $B_\Theta = 0$ and $E_\Theta = 0$ and analyze successively these 3 equations.

<u>The 3rd equation</u> of (A-2) describes the longitudal acceleration. The accelerating force is provided by E_z, the longitudinal electric field and by two other terms linked to the magnetic field. The term $\dot{r}\,B_\Theta$ is null because we have assumed $B = 0$. The second term $-\,q\,r\,\dot{\Theta}\,B_r$ combines the tangential velocity $r\,\dot{\Theta}$ and the radial field B_r.

The radial field B_r is null on the axis by symmetry and therefore small at the vicinity of the axis, so that this term is usually neglected (for example with B_r = 100 Gauss at 1 cm and $\frac{\theta}{2\pi}$ = 1 GHz the effect is equivalent to an electric field of 1 kV per meter, negligible with respect to the accelerating field E_z is usually of several MV per meter).

This third equation therefore reduces to

$$\frac{d}{dt} = (m\,\dot{z}) = q\,E_z \qquad \text{(A-3)}$$

This equation is however relativistic ($m = \gamma\, m_0$) so that it takes some precaution to integrate since γ is a function of time. The equation can be written to express the time variation of γ.

$$m_0 c \frac{d}{dt} \ (\beta\gamma) = q\,E_z$$

or using the usual relativistic formulae [13]

$$\dot{\gamma} = \beta q \frac{E_z}{m_o c} \qquad \text{(A-4)}$$

<u>The second equation</u> (A-2) provides the "Bush theorem". We can rewrite it under the integral form

$$mr^2\dot{\theta} = \frac{g}{2\pi} \int 2\,\pi r\,(\dot{z}B_r - \dot{r}B_z)\,dt \qquad \text{(A-5)}$$

The quantity $2\,\pi r\,(\dot{z}B_r - \dot{r}B_z)dt$
can be written

$$2\,\pi r\,(B_r dz - B_z dr).$$

If we note Ψ the flux through the circle of radius r (fig. 15) we see that the flux $2\pi r B_r dz$ has escaped and the flux $2\pi r B_z dr$ has been added, in other words

$$d\Psi = 2\pi r\,(B_z dr - B_r dz)$$

that we can insert in (A-5) to obtain

$$\dot{\theta} = -\frac{g}{m}\frac{1}{2\pi r^2} \ (\Psi - \Psi_o)$$

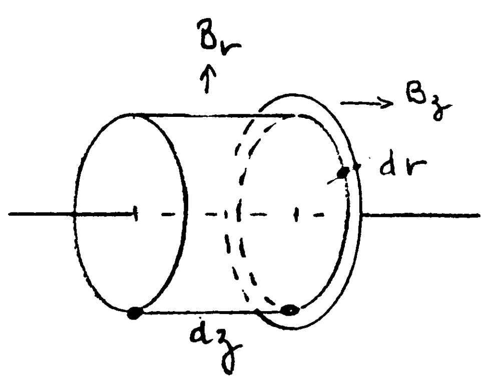

Figure 17

where Ψ_o is the flux in the circle of radius r at a place where $\theta \doteq 0$.

If one adds the assumption that the field B_z is constant through the circle of radius r this equation takes the form

$$\dot{\Theta} = -\frac{q}{2m}\left[B_z - \frac{\Psi_o}{\pi r^2}\right] \qquad \text{(A-6)}$$

and is called the "Bush theorem", it is used in the discussion of what happens in a solenoid field.

The value of $\dot{\Theta}$ is half the cyclotron frequency in the field B_z if $\Psi_0 = 0$, it is therefore very high, for example if B_z = 100 gauss and with a non relativistic electron ($|\frac{e}{m}| = 1.8\ 10^{11}$ C.kg^{-1}). The frequency is approximately 1 GHz.

<u>The first equation</u> will provide the paraxial equation, that is the evolution of r with time. It requires however a few manipulations.

We first remark that $B_\Theta = 0$ and use $\dot{\Theta}$ given by the Bush theorem to write

$$\frac{d}{dt}(m\dot{r}) = q\,E_r - \frac{q^2 \cdot r}{4m}\left[B_z^2 - \left[\frac{\Psi_0^2}{\pi r^2}\right]^2\right] \qquad \text{(A-7)}$$

The second step is to develop the lefthand term and replace m by γm_o

$$\frac{d}{dt}(m\dot{r}) = \dot{\gamma} m_o \dot{r} + \gamma m_o \ddot{r} = \gamma m_o\left[\ddot{r} + \frac{\dot{\gamma}}{\gamma}\dot{r}\right]$$

or using eq. A4.

$$\frac{d}{dt}(m\dot{r}) = \gamma m_o\left[\ddot{r} + \frac{\beta q}{\gamma m_o c} E_z \dot{r}\right]$$

so that the A-7 equation can be written

$$\ddot{r} + \frac{\beta q}{\gamma m_o c} E_z \dot{r} + \frac{q^2 B_z^2}{4\gamma^2 m_o^2} r - \frac{q^2 \Psi_o^2}{4\pi^2\gamma^2 m_o^2}\frac{1}{r^3} - \frac{qE_r}{\gamma m_o} = 0 \qquad \text{(A-10)}$$

that is equation 2.10 of Lawson [5], using the same notations. It is the paraxial equation with time as independent variable.

The paraxial equation with space as independent variable can be deduced from (A-10). A certain number of manipulations are again required.

We use

$$\dot{r} = \frac{dr}{dt} = \frac{dr}{dz}\frac{dz}{dt} = \beta c\, r'$$

where the prime denotes derivation with respect to z and in a similar way

$$\ddot{r} = \frac{d}{dt}(\beta c r') = r''\beta^2 c^2 + r'\beta'\beta c^2$$

so that we can rewrite the two first terms of equation A-10

$$\ddot{r} + \frac{\beta q E_z}{\gamma m_0 c}\dot{r} = \beta^2 c^2 \left(r'' + \frac{\beta'}{\beta} r' + \frac{\gamma'}{\gamma} r'\right)$$

Since $\quad \frac{\dot{\gamma}}{\gamma} = \frac{\beta q E_z}{\gamma m_0 c} \quad$ and $\quad \gamma' = \dot{\gamma}\beta c$

that is $\quad \ddot{r} + \frac{\beta q E_z}{\gamma m_0 c}\dot{r} = \beta^2 c^2 \left(r'' + \frac{1}{\beta^2}\frac{\gamma'}{\gamma}\right)$

so that A-10 can be rewritten

$$r'' + \frac{1}{\beta^2}\frac{\gamma'}{\gamma} r' + \left[\frac{qB_z}{2\beta\gamma m_0 c}\right]^2 r - \left[\frac{q\Psi_0}{2\pi\beta\gamma m_0 c}\right]^2 \frac{1}{r^3} - \frac{qE_r}{\beta^2\gamma m_0 c^2} = 0 \qquad \text{(A-11)}$$

In the absence of space charge a simplified version of this equation can be derived. Since the radial field E_r can be derived from the longitudinal field E_z through

$$\mathrm{div}\,\vec{E} = 0$$

that is, in cylindrical coordinates and with $E_\Theta = 0$

$$\frac{1}{r}\frac{\partial}{\partial r} rE_r + \frac{\partial}{\partial z} E_z = 0$$

or, assuming a linear variation of E_r at the vicinity of the axis

$$E_r = -\frac{1}{2} r E_z'$$

that is using A-4

$$E_r = -\frac{1}{2} r\gamma'' m_0 c^2/q$$

The new version of the paraxial equation is then

$$r'' + \frac{\gamma' r'}{\beta^2\gamma} + \frac{\gamma''}{2\beta^2\gamma} r + \left[\frac{qB_z}{2\beta\gamma m_0 c}\right]^2 r - \left[\frac{q\Psi_0}{2\pi\beta\gamma m_0 c}\right]^2 \frac{1}{r^3} = 0 \qquad \text{(A-12)}$$

Finally it is possible to express this equation under a different form if one notes that the values of γ and β can be linked to the variation of potential ϕ in the gap and to the rest energy of the electron expressed by the potential ϕ_o

$$\phi_o = - \frac{m_o c^2}{q}$$

$$\gamma = 1 + \frac{\phi}{\phi_o}$$

$$\beta^2 = \frac{\phi(2\phi_o + \phi)}{(\phi + \phi_o)^2}$$

The equation then takes the form that we have used in the text

$$\frac{\phi(2\phi_o+\phi)}{(\phi_o + \phi)} r'' + \phi' r' + \left[\frac{\phi''}{2} - \left(\frac{qB_z}{2m_o c}\right)^2 \frac{\phi_0^2}{\phi+\phi_0}\right] r + \left[\frac{q\psi_o}{2\pi m_o c}\right]^2 \frac{\phi_0}{\phi+\phi_o} \frac{1}{r^3} = 0 \qquad \text{(A-13)}$$

which is equation 2-16 of Lawson [5] with the same notation.